

FEASIBILITY STUDY ON LONG-SPAN CLT-GLULAM COMPOSITE FLOORING SYSTEM CONNECTED WITH BAMBOO-TENON SHEAR CONNECTORS

Yue Diao¹, Cristiano Loss²

ABSTRACT: The rise of cross-laminated timber (CLT) became a cornerstone for the development of mass timber high-rise buildings and for large applications of timber products in construction. The design of CLT floors is often hinged upon meeting the vibration and deflection requirements under serviceability limit states. As a result, thick and material-intensive sizes of floor members can result from the design to fulfil the minimum stiffness requirements.

A long-span composite flooring system made of CLT panel and glulam ribs is a structurally optimized and cost-effective solution. In this paper, a feasibility study of a 12-meter composite flooring system consisting of CLT slab and glulam ribs jointed through bamboo-tenon shear connectors was conducted. The flooring system was designed to achieve performance objectives per the National Building Code of Canada, focusing on office spaces. Finite element modelling was used to investigate the behaviour of connectors under push-out shear forces. A parametric study of the shear connector was then carried out. Impacts of the material properties of mortise-tenon on the behaviour of the joints were discussed. Further, the structural performance of the composite system was investigated under several case scenarios. Specific design recommendations for adopting bamboo-tenon as the shear connector in composite systems were provided.

KEYWORDS: Bamboo connectors, CLT composites, flooring systems, long-span floors

1 INTRODUCTION

1.1 COMPOSITE FLOORING SYSTEMS

The acceptance of composite flooring systems started with the growth of reinforced concrete-based and concrete-steel composite floors. In Europe, design provisions of such composite floors have been included in Eurocode 4 [1]. More recently, research has been conducted with the aim of replacing concrete slabs with CLT panels. With specific reference to the timber-timber floor composites, general design guidelines of a fully connected CLT-glulam ribbed system have been discussed in the proceeding of the joint Conference of COST Action [2]. Several long-span timber floor solutions using inclined self-tapping screws as shear connectors have been studied in Europe [3]. Research has been conducted to investigate new connection systems; the result of metal fastener combinations employed in timber composite floor structures can be founded in [4]. It has been shown that these mechanically connected composites can be designed assuming full composite action. However, with the increase in floor span, the number of metal fasteners used, the on-site labor costs and the construction time increase along with it, making larger span timber flooring systems less attractive in practice.

Therefore, there is an urge to develop high-structural performance connection systems for timber composite floor systems.

1.2 MODERN CARPENTRY JOINTS

The advancement of automation technologies in the wood industry, namely computer-numerically-controlled (CNC) machining technology, increased the level of prefabrication of CLT structures. As a result, CLT panels can be manufactured as wall and floor elements and quickly assembled on-site. These technologies also increased the possibility of using CNC machining carpentry joints to serve as the connection system in mass timber construction. Studies of carpentry joints used in modern timber frame structures have been conducted by Tannert et al. [5] and Claus and Seim [6]. More recently, the castellation CLT joints have been studied by Brown et al. [7]. Schmidt and Blass [8] have investigated the behavior of hardwood connectors serving as in-plane shear connectors for CLT walls.

1.3 ENGINEERED BAMBOO PRODUCTS

Bamboo is a rapidly renewable biomaterial with similar environmental benefits and mechanical properties as timber. Full culm bamboo can be applied as a structural

¹ Yue Diao, Sustainable Engineered Structural Solutions Laboratory, Department of Wood Science, University of British Columbia, Canada, yuediao@mail.ubc.ca

² Cristiano Loss, Sustainable Engineered Structural Solutions Laboratory, Department of Wood Science, University of British Columbia, Canada, cristiano.loss@ubc.ca

material in low-rise residential housings in countries with rich bamboo resources, such as the Philippines, Colombia, Ecuador, China, and India. In recent years, significant efforts have been devoted to the characterization of the mechanical properties of engineered bamboo products, such as laminated bamboo lumber (LBL), parallel strand bamboo (PSB), and bamboo laminated veneer lumber (BLVL), aiming to expand their application as load-bearing members in buildings and eventually, incorporate them into the building code. However, other factors of using bamboo material in the built environment must be addressed, such as the fire protection strategy, the connection design approach, and its long-term behaviour.

1.4 OBJECTIVES

Seeing the technological developments in the wood industry and needs for a sustainable building environment, this paper aims to develop an engineered bamboo shear connectors for wood composite floorings. Due to enhanced mechanical properties of engineered bamboo, it is anticipated that such bamboo-tenon connectors are suitable candidates for CLT-glulam floors intended for long-span usage. Besides, the design value of the bamboo-tenons remains in the elastic region, aiming to prevent the irreversible damage in local areas of timber members for future deconstruction and reconstruction purpose.

2 CLT-GLULAM RIBS COMPOSITE FLOORING SYSTEM CONNECTED WITH BAMBOO SHEAR CONNECTORS

2.1 CLT-GLULAM FLOOR

A 12-meter timber composite flooring system consisting of a 3-ply CLT panel and glulam ribs connected by bamboo-tenon shear connectors was designed to fulfil the static performance objectives per the National Building Code of Canada (NBCC) [9]. A non-structural concrete topping was placed on top of the CLT panels and counted as dead load only. The flooring system was modular designed, assumed sitting on continuous mass timber vertical load-bearing elements or hybrid timber-based frameworks. The structural elements are illustrated in Figure 1.

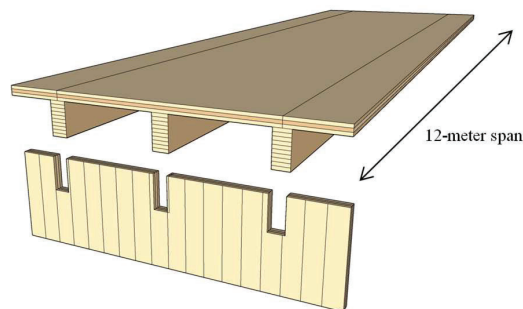


Figure 1: CLT-glulam composite flooring and its end supports

2.2 BIO-BASED TENON-TYPE SHEAR CONNECTORS

The three-piece tenon-type shear connector requires grooving into both the CLT and glulam ribs and is made of engineered bamboo products, as shown in Figure 2.

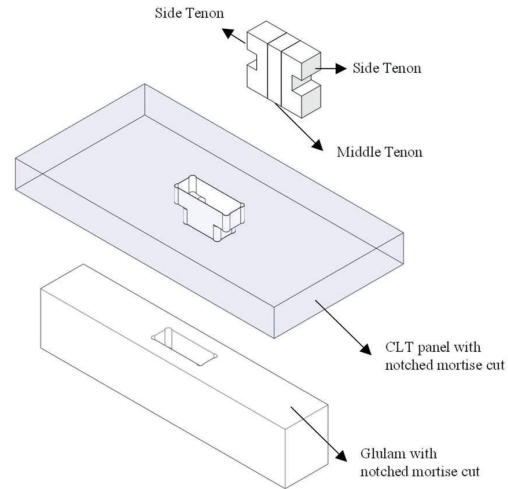


Figure 2: Three-piece bamboo-tenon shear connector and CLT-glulam with mortise cuts

The geometry of the tenon was inspired by the traditional joinery technique combined with CNC-machined carpentry joints used in modern timber structures. The sides of the tenon are symmetrical pieces with grooved profiles to accommodate CLT panels. The middle piece is used for tightening the mortise-tenon joint. The entire connector is embedded in mass timber members and covered by non-structural floor components, as described in Section 2.1. The corners of mortises in CLT and glulam were routed as rounded circles (i.e., notches in the figure). It is a feature of modern CNC machine drilling and provides a buffer area at the corner of the mortise-tenon contact region. Two engineered bamboo products were considered for the tenon material in this study, e.g., parallel strand bamboo (PSB) and laminated bamboo lumber (LBL).

3 MODELLING IN ANSYS

3.1 MATERIAL PROPERTIES

Mass timber products in this study, i.e., CLT and glulam, were modelled using solid wood properties and assembled by layer's fibre orientation. Wood is assumed as an orthotropic material. The material properties of PSB and LBL were described using the transversal isotropic and orthotropic models, respectively. This difference is caused by their different processing procedure [10]. The fibre orientation of each material and corresponding axis directions in the modelling space are shown in Figure 3.

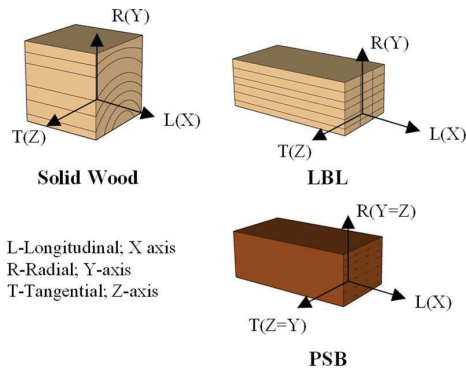


Figure 3: Biomaterials fibre orientations and their axes in Cartesian coordinate system

The elastic properties of wood were obtained from Wood Handbook [11]. The species of CLT and glulam are spruce (Sitka) and Douglas-fir, respectively. For details see authors' previous work [12]. The elastic properties of bamboo products are listed in Table 1 and Table 2, while more details can be found in [13, 14] and [15, 16] for PSB and LBL, respectively.

Table 1: Elastic modulus of engineered bamboo products

Product	E_x	E_y	E_z	G_{xy}	G_{xz}	G_{yz}
PSB	11890	3066	3066	1361	1361	746
LBL	9391	1440	1149	1365.08	1260.09	461.81

*Unit in Mpa

Table 2: Poisson ratios of engineered bamboo products

Product	μ_{xy}	μ_{xz}	μ_{yz}
PSB	0.411	0.411	0.115
LBL	0.25	0.2	0.42

Material properties under compressive and shear forces are the decisive parameters in tenon-type contact joints. Summarizing from [13-17], the constitutional law of wood and bamboo product is illustrated in Figure 4. It should be noticed that the stress-strain relationship of wood material under complex stress was well established for modelling with entire curve behaviour. In contrast, the studies on the stress-strain relationship of bamboo products most focus on describing the curve before failing.

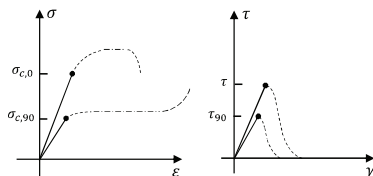


Figure 4: Stress-strain relationship under compression and shear

The bilinear isotropic hardening model is assumed to describe the behaviour of wood and engineered bamboo

products in the plastic phase. Table 3 lists the tangent modulus of wood in compression, validated by the mean values of clear wood specimens from [18] and [19] for spruce CLT species and Douglas-fir glulam species, respectively. The tangent modulus and strengths of PSB and LBL under compression and shear forces were obtained from the mean value results from [13-14] and [15-16], respectively. σ_{xx} , σ_{yy} and σ_{zz} are the normal stresses; σ_{xy} , σ_{yz} and σ_{xz} are the shear stresses.

Table 3: Properties in the plastic region (unit in Mpa)

Item	CLT, Spruce	Glulam, D.-Fir	PSB, Moso	LBL, Moso
$E_{Tangent}$	123.20	149.60	2853.60	93.91
σ_{xx}	37.80	50.00	33.09	46
σ_{yy}	4.1	6.0	7.68	21.63
σ_{zz}	4.1	6.0	7.68	19.62
σ_{xy}	4.08	5.7	23.44	18.13
σ_{yz}	0.93	1.9	3.64	22.59
σ_{xz}	2.85	3.99	23.44	6.58

The Hill criterion, given in Equation (1), was applied as the failure criteria:

$$f(\sigma) = \sqrt{\frac{F(\sigma_{yy} - \sigma_{zz})^2 + G(\sigma_{zz} - \sigma_{xx})^2}{+H(\sigma_{xx} - \sigma_{yy})^2 + 2L\sigma_{yz}^2 + 2M\sigma_{zx}^2 + 2N\sigma_{xy}^2}} \quad (1)$$

F, G, H, M, and N are material constants from the tests, defined by Equation (2)-(7):

$$F = \frac{1}{2} \left(\frac{1}{R_{yy}^2} + \frac{1}{R_{zz}^2} - \frac{1}{R_{xx}^2} \right) \quad (2)$$

$$G = \frac{1}{2} \left(\frac{1}{R_{zz}^2} + \frac{1}{R_{xx}^2} - \frac{1}{R_{yy}^2} \right) \quad (3)$$

$$H = \frac{1}{2} \left(\frac{1}{R_{xx}^2} + \frac{1}{R_{yy}^2} - \frac{1}{R_{zz}^2} \right) \quad (4)$$

$$L = \frac{3}{2} \left(\frac{1}{R_{yz}^2} \right) \quad (5)$$

$$M = \frac{3}{2} \left(\frac{1}{R_{xz}^2} \right) \quad (6)$$

$$N = \frac{3}{2} \left(\frac{1}{R_{xy}^2} \right) \quad (7)$$

R_{ij} are the yield stress ratios, defined by Equation (8):

$$R_{11} = \frac{\sigma_{xx}^y}{\sigma_y}; R_{11} = \frac{\sigma_{yy}^y}{\sigma_y}; R_{11} = \frac{\sigma_{zz}^y}{\sigma_y}; R_{11} = \sqrt{3} \frac{\sigma_{xy}^y}{\sigma_y}; R_{11} = \frac{\sigma_{yz}^y}{\sigma_y}; R_{11} = \frac{\sigma_{xz}^y}{\sigma_y} \quad (8)$$

Assuming the compressive strength in the main fibre direction as the reference yielding stress, σ_y , the generated yield stress ratios are listed in Table 4.

Table 4: Yield stress ratios

Item	CLT, Spruce	Glulam, D.-Fir	PSB, Moso	LBL, Moso
R_{11}	1.00	1.00	1.00	1.00
R_{22}	0.11	0.12	0.23	0.47
R_{33}	0.11	0.12	0.23	0.43
R_{12}	0.19	0.20	1.23	0.68
R_{23}	0.04	0.07	0.19	0.85
R_{13}	0.13	0.14	1.23	0.25

3.2 MODELLING AT THE JOINT LEVEL

One-meter-long solid-type joint models were built in the ANSYS workbench to investigate the joint shear performance under static push-out force. See Figure 5.

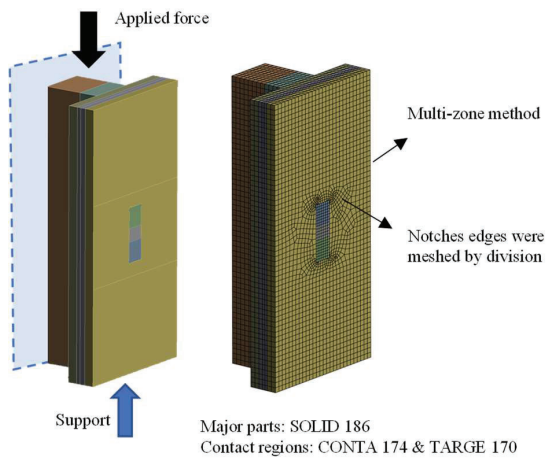


Figure 5: Joint model

CLT panel was modelled by layers bonded together. The crosswise layout was defined by a local coordinate system. Glulam was built as one united body and its material properties were defined by the global coordinate system. Both members were split locally to improve the meshing quality around the mortise. The tenon was orientated with the main fibre direction perpendicular to the shear force direction with a specific defined local coordinate system. Solid 186 element was employed in all bodies. The multizone meshing method was applied. To capture the mortise-tenon in detail, the meshing size around the contact area was refined. The mortise notch edges were divided into 5 segments. Face meshing was applied to the tongue of the CLT panel. The global and local meshing sizes were compatible and chosen for a high-quality finite-element meshing result. The overall meshing size of CLT and glulam were set as 18 mm whereas the meshing size of the tenon was set as 15 mm. The meshing quality was 0.94 on the average, with all the components meshed using hex elements.

The surface element was used to evenly distribute applied force to the loading area. Sub-steps were set for convergence after approaching the plastic region of materials. In sub-step 1 to 4, the force increment is 20 kN. After applying 80 kN to the model, 10 kN was applied per sub-step until the finish. Large deformation was allowed. A frictional coefficient of 0.5 was applied to all the contact surfaces within the model [20].

The parametric study was conducted to investigate the joint performance when varying material combinations of tenons and contact characteristics between tenon pieces. The studied schemes are listed in Table 5.

Table 5: Parametric study scheme

Scheme No.	Side Tenon	Middle Tenon	Contact
1	PSB	PSB	Bonded
2	PSB	PSB	Frictional
3	PSB	LBL	Frictional
4	LBL	LBL	Bonded
5	LBL	LBL	Frictional
6	LBL	PSB	Frictional

Note: Contact refers to between tenon pieces

3.3 MODELLING AT THE FLOOR LEVEL

The CLT-glulam rib flooring system was modular designed where one floor module consists of one CLT slab with dimensions of 105 × 1200 × 12000 mm (thickness × width × length) and one glulam with dimensions of 175 × 380 × 12000 mm (width × depth × length). Single floor module was built in ANSYS Workbench adjusting the modelling method used for the joint, with minor changes on meshing. The variation of timber products caused by its defects and product assembly process are not considered in this stage of investigation. However, to better capture the structural behaviour at the system level, the meshing size of the fully and not connected composite beams was set as 60 mm. This was compared with the theoretical results of applying the Gamma method to a simply supported CLT-glulam composite floor of the same configuration. Bonded contact was applied between CLT and glulam under fully connected situations, whereas frictional contact was applied for not structurally connected composite floors. The same frictional coefficient as the joint model was used. The proposed bamboo-tenon connected flooring system was built based on geometry imported from SolidWorks. The as-built floor models are shown in Figure 6.

The case study was conducted using the loading conditions listed in Table 6. The impact of supporting systems on the structural behaviour was studied, considering common office space usage; see cases 1 to 3. In these cases, a specified live load of 2.4 kpa is uniformly distributed on the floor. The serviceability of the proposed flooring system was compared under 1.0 DL + 1.0 LL load combinations. Extreme loading conditions, as per Notes A-Table 4.1.5.3 of NBCC, were also studied. Such cases as using proportions of the long-span floor as

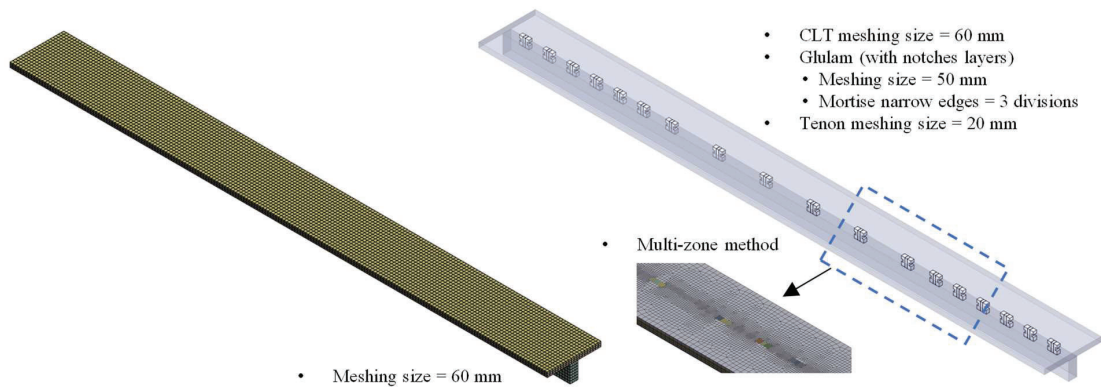


Figure 6: Finite-element models of one module CLT-glulam composite floor (Left: full and not connected floor; right: proposed floor)

Table 6: Case studies of the flooring system

Loads	Boundary conditions and loading areas
Uniformly distributed loads, q : 1.0 DL +1.0 LL	Case 1: Simply support q
	Case 2: Fix-Roller q
	Case 3: Fix Ends q
Uniformly distributed loads, q : 1.25 DL +1.5 LL	Case 4: Simply support q
	Case 5: Extra LL in the middle segments q'
Uniformly distributed loads, q : 1.25 DL +1.5 LL Partially distributed load, q' : 1.5 LL	Case 6: Extra LL at both ends q'
	Case 7: Extra LL at one end q'

a temporary storage room for files or furniture. In these cases, an extra live load of 2.4 kpa was partially distributed on segments of the flooring system. See cases 4 to 7. The 12-meter span floor is divided into 4 segments of 3 meters. The flexural behaviour of the proposed composite flooring system under ultimate limit states and extreme loading conditions were investigated.

4 RESULTS AND DISCUSSION

4.1 LOAD-SLIP CURVES OF THE JOINT

Figure 7 shows the load-slip responses of the parametric study results extracted from the joint models at varying of the design scheme. The estimated elastic stiffness of the joints is specified in Table 7.

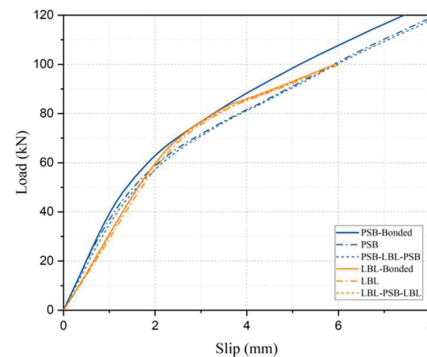


Figure 7: Extracted load-slip responses

Table 7: Stiffness results of tenon joints

Scheme No.	Tenon Configuration*	Stiffness (kN/mm)
1	PSB-Bonded	39.62
2	PSB	36.73
3	PSB-LBL-PSB	34.46
4	LBL-Bonded	30.89
5	LBL	29.11
6	LBL-PSB-LBL	30.69

*Side-middle-side tenon material

In schemes 1 to 3, PSB is designed to be directly in contact with the timber members. On the contrary, schemes 4 to 6 employ LBL as the side tenons in contact with the CLT and glulam members.

Within the PSB tenon groups, i.e., scheme 1 to 3, the internal bonded group hindered the sliding between tenon components, resulting in an increase of 8% on the overall

stiffness result compared to the pure PSB tenon group. The same effect occurs in the LBL-bonded and LBL groups, which shows a 6% increase of the stiffness. When changing the middle tenon material from PSB to LBL, i.e., from scheme 2 to scheme 3, the joint stiffness reduces by 21 % due to lowering the stiffness of the middle tenon. Interestingly, by changing the middle tenon from PSB to LBL, i.e., from scheme 5 to 6, the stiffness increased by 5%, closing to the bonded group (scheme 4). The stress distributions under different loads are plotted in Figure 8.

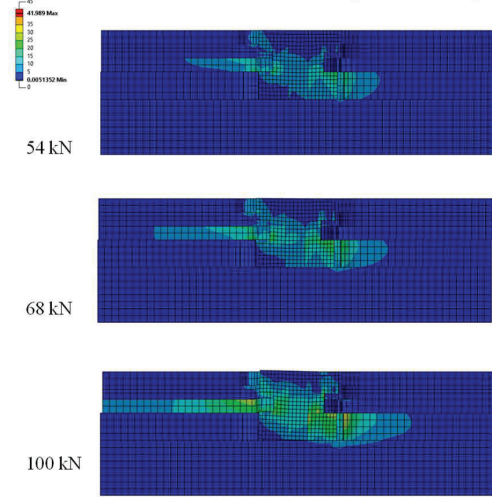


Figure 8: Von-mises stress distribution of LBL-PSB-LBL tenon

4.2 IMPLEMENTATION OF BAMBOO-TENON TO THE LONG-SPAN COMPOSITE FLOORING SYSTEM

By analysing the joint response under push-out shear forces, the LBL-PSB-LBL tenon (scheme 6) was selected for the proposed CLT-glulam flooring application. The proportional limit of 54 kN from the load-slip curves was assumed as the joint capacity. The flooring system was divided into three segments assuming different connectors spacing in each, in order to simplify the installation of the shear connectors. The amount and spacing of selected bamboo-tenon shear connectors are illustrated in Figure 9, and details are summarized in Table 8.

Table 8: Bamboo-tenon distribution along the beam

Segment	Starting point	Ending point	Amount per meter	Spacing	Edge distance
1	0	3000	2	300	300
2	3000	9000	1	800	400
3	9000	12000	2	300	300

Unit in mm

The composite efficiency of the proposed composite floor was investigated using Equation (9).

$$\eta = \frac{(EI)_{ef} - (EI)_0}{(EI)_{\infty} - (EI)_0} \quad (9)$$

Where $(EI)_{ef}$, $(EI)_0$ and $(EI)_{\infty}$ represent the effective bending stiffness from the proposed bamboo-tenon shear connector jointed composite flooring system, not connected composite floor and the fully connected composite floor, respectively.

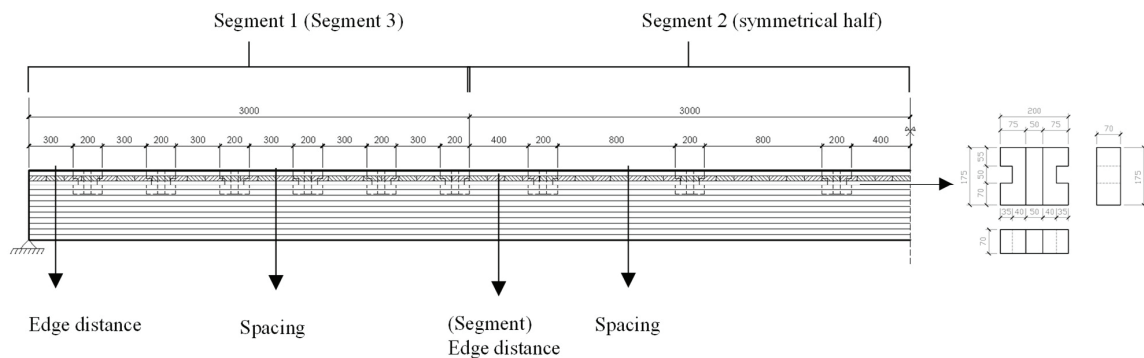


Figure 9: Bamboo-tenon shear connector connected CLT-glulam composite floor

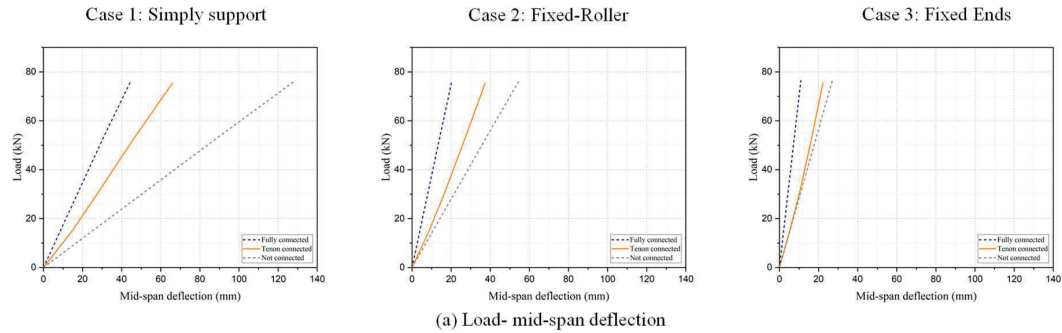
4.3 CASE STUDIES OF THE COMPOSITE FLOOR UNDER SERVICEABILITY DESIGN

Figure 10 shows the case study results on the composite flooring system under serviceability loads (case study 1 to 3 in Table 6). All case scenarios were loaded to the prescribed loads. In the simply supported composite floor (case 1), the composite efficiency of the proposed flooring system is 50.79%. The supporting conditions significantly influenced the composite efficiency of the composite floor. Fixed support in this study has limited both the

translations and rotations of the floor end elements. By moving into restrained supports, the differences in deflection between the floor with no and full composite action was shown reduced. Specifically, the composite efficiency of floors with fix-roller supports and the fixed ends support were 27.41 % and 14.69%, respectively. These indicate the benefits of implementing shear connectors become less remarkable when increasing the restriction from the supporting system.

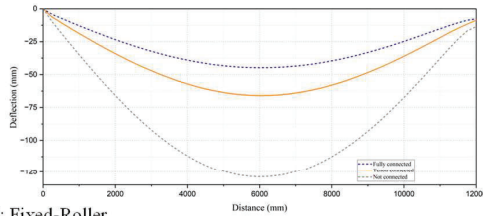
A construction path was created on the CLT-glulam interface, going through the central line of the glulam top surface and penetrating through tenons if implemented. The shear stresses on the interface are plotted in Figure 10, (c). With tenons inserted, the shear stress on the interface shows an oscillating pattern, i.e., the stress increases when passing through a tenon, reaches the regional maximum value at the contact surface of mortise-tenon and decreases to zero when moving to the area where no tenon is inserted. For example, in case 1, the

regional peak stress value occurs at 500 mm from the edge, which is also the end of the first inserted tenon. Also in case 1, the regional peaks value along the span shows the same decreasing trend as fully connected composite beams, i.e., the regional peak value keeps declining when approaching the mid-span of the floor. By changing the degrees of freedom at the supports, the maximum stress moved from the first tenon area to the 6th and the 5th tenon in the fix-roller and the fixed ends cases, respectively.

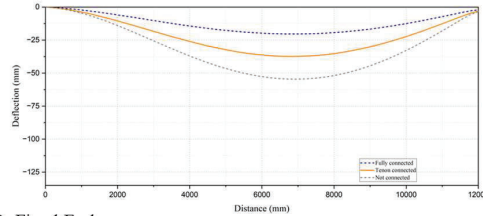


(a) Load- mid-span deflection

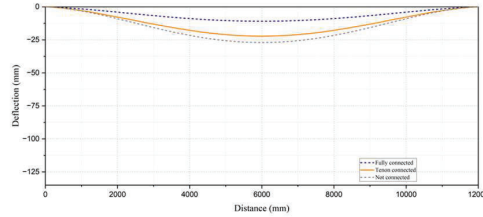
Case 1: Simply support



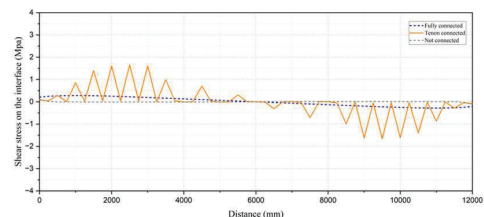
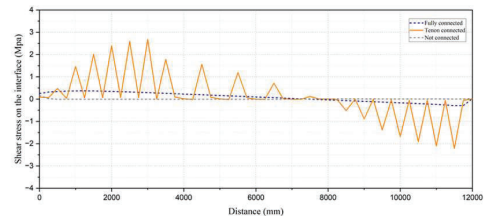
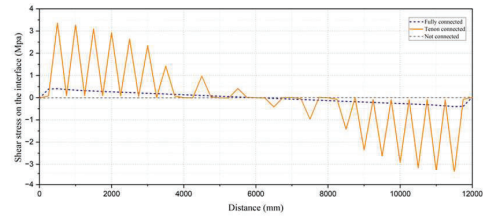
Case 2: Fixed-Roller



Case 3: Fixed Ends



(b) Deflection along the span



(c) Shear stresses on the interface

Figure 10: Comparison on the flexural performance of the composite floors with different boundary conditions under serviceability loading conditions

Figure 11 shows the case study results of long-span composite floors with extra partially distributed live loads with loading conditions listed in Table 6. The case study models were loaded to the design load as described in Table 6, case 4 to 7. A yielding point can be observed on the load-deflection curves. It should be noticed that this is caused by the deformation near the supporting area.

Evidence can be found from the deflection along the beam curves, where a kink appeared near the supports. The stress distribution of the composite flooring system plotted in Figure 12 also illustrates this deformation. Besides, stress results were checked on all structural members. It shows all members remain in their elastic regions under the design value.

Compared to the simply supported with uniformly distributed loads case (case 1), the shear stress increased at the increasing of live load on the floor segments in other cases. For example, when adding an extra 2.4 kpa live load to each end, the peak shear stress increased from 4.16 Mpa in case 1 to 4.42 Mpa in case 6.

Among three extreme loading case scenarios, the extra live loading area on the middle segments causes more deflection of the structure and overall shear stresses on the interface. Therefore, this case scenario should be seen as the least favourable scenario under extreme loading conditions.

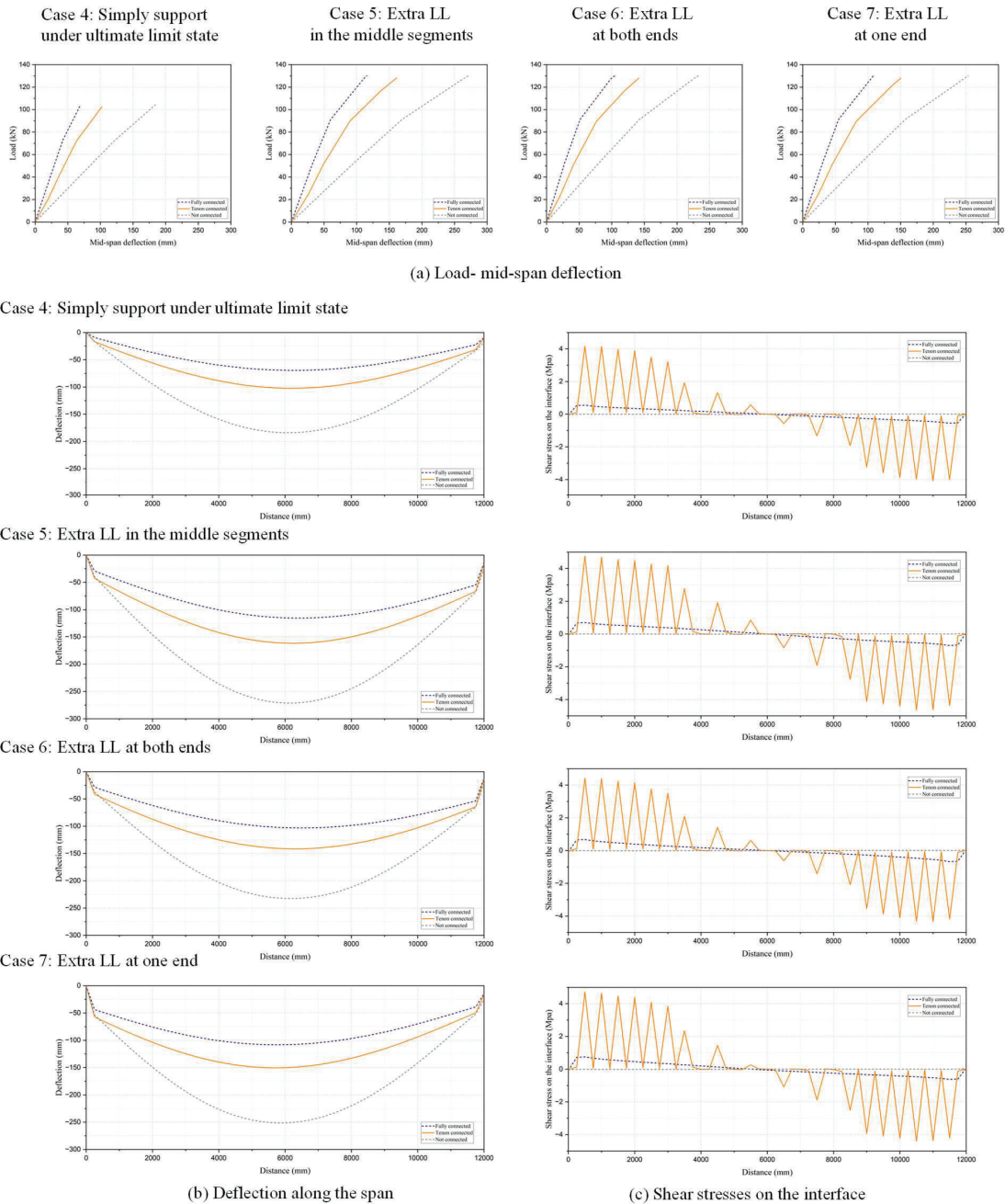


Figure 11: Comparison on the flexural behaviour of the composite floors under ultimate limit state and extreme loading conditions

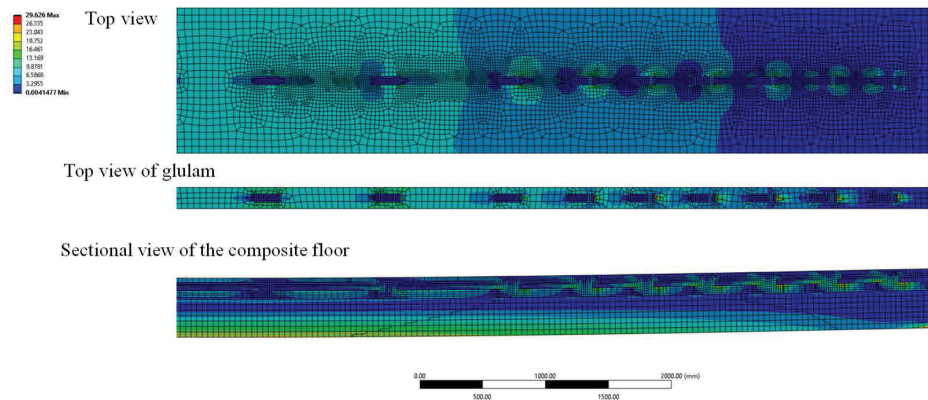


Figure 12: Von-mises stress distribution of bamboo-tenon connected composite floor under ultimate limit state (half span, case 4)

5 OVERVIEW

5.1 COMPARISON BETWEEN THE ANALYSIS AT THE JOINT LEVEL AND THE FLOOR LEVEL

The geometric feature of the bamboo-tenon, i.e., the tongue-and-groove cut, was generated for the purpose of quick assembly and disassembly. In one of the preliminary FEM simulations at the joint level, where bonded contact was applied to all the contact surfaces within the mortise-tenon, a quick distortion occurred on the glulam notches edge and the tongue of CLT panels, indicating the potential decrease of the overall joint capacity due to the existence of glue. Within the parametric study scope of this study (Table 5), the comparison between internal glued joint groups and the frictional connected joints showed a limited increase in the joint stiffness by internal bonding. Considering the costs of adhesives and the curing time, the internal glued joint was not chosen for the subsequent floor design.

However, the rotational behaviour of the tenon has a more significant impact on the global flexural behaviour when implemented in the long-span CLT-glulam flooring system. When the composite system undergoes deformation under bending, the rotational behaviour of the tenon leads to a detached mortise-tenon surface at the bottom. Therefore, the proposed tenon-type shear connector failed to efficiently transfer the forces between members as anticipated. A much lower composite efficiency is witnessed when analysing the proposed bamboo-tenon connected long-span composite floor.

This inconsistent results between the joint and the floor models indicates that special attention needs to be drawn to the rotational behaviour of tenon-type connectors. Specifically, tenon geometries and shape can be redefined with a new design to minimize the rotation of the bamboo-tenon under shear forces.

5.2 COMPARISON BETWEEN PROPOSED CONNECTOR AND SELF-TAPPING SCREWS

CLT construction using self-tapping screws as connectors has been studied and well implemented in practice. In the 7-meter CLT ribbed composite system studied by [21], 48

screws were used to engage floors with full composite action. For longer spans, the number of screws and can be around 80 to 90 [22]. In general, high level of composite action is guaranteed by reducing spacing of screws, as demonstrated by [23].

Using a specific selection of material combination, the number of shear connectors used to assemble a 12-meter flooring system can be as low as of 18 bamboo-tenons. Besides, the fabrication tolerance can be precisely controlled in the factory. As such, the proposed tenon-type connectors of this study demonstrate a structurally efficient solution.

5.3 LIMITATIONS OF MODELLING

Compared to the well-established knowledge on the behaviour of wood, the lack of harmony material testing methods on engineered bamboo products and reliable dataset of their mechanical properties led to uncertainty in the estimation of the bamboo-tenon connector capacity. Besides, future modelling will benefit from the experimental test results of the joints, as well as the full-scale flooring tests. Limited by the knowledge and experimental database of the structural behaviour of tenon-type shear connectors, 3D floor models were used in this study. Further study can advance this modelling method by incorporating reliability analysis on the impacts of defects on the mechanical properties of structural members.

6 CONCLUSION

This paper mainly investigated the structural performance of a bamboo-tenon shear connector jointed long-span CLT-glulam ribbed composite flooring system. Specific recommendations for the bamboo-tenon design are concluded as follows:

1. Having a stiffness of 30.69 kN/mm per tenon per joint and an elastic capacity of 54 kN under shear forces, the LBL-PSB-LBL tenon material combination is recommended for this three-piece tenon design;
2. A total number of 18 bamboo-tenon were implemented by segments in the proposed composite flooring system; however, the

rotational behaviour of the tenon reduced the composite efficiency;

3. By increasing the restrains of supports on the composite flooring system, the variance in the flexural behaviour of floors under full and non-composite action was shown reduced, resulting in less composite efficiency when implementing shear connectors;
4. Under extreme loading conditions, the extra live load partially distributed on the middle segments should be concerned as the worst-case scenario and should be prioritized.

This feasibility study demonstrates the potential of using bamboo-tenon as shear connector in CLT-glulam long-span flooring systems. Further optimization of the bamboo-tenon is needed. This research helps broaden the applications of engineered bamboo products in the future building environment.

ACKNOWLEDGEMENT

This research was financed by the Natural Sciences and Engineering Research Council (NSERC) of Canada through the Discover Program, grant number RGPIN-2019-04530, and Discovery Launch Supplement, grant number DGEGR-2019-00265. MOSO® Bamboo company is acknowledged as the engineered bamboo products sponsor in this study. The State Scholarship Fund of China, No. 202006510006, awarded to Yue Diao, is also acknowledged.

REFERENCES

- [1] Committee of European Normalisation (CEN). EN 1994-1-1-2004, Eurocode 4: Design of composite steel and concrete structures, Part 1–1 General Rules and Rules for buildings 1994–2005.
- [2] A. Thiel, R. Brandner. ULS Design of CLT Elements –Basics and Some Special Topics. In: Joint Conference of COST Actions FP1402 & FP1404 KTH Building Materials, 65-90, 2016.
- [3] P. Papastavrou, S. Smith, T. Wallwork, A. McRobie, N. Niem. The Design of Cross-Laminated Timber Slabs with Cut-Back Glulam Rib Downstands-From Research to Live Project. In: WCTE, 2016.
- [4] N. Jacquier. U. A. Girhammar. Evaluation of Bending Tests on Composite Glulam–CLT Beams Connected with Double-Sided Punched Metal Plates and Inclined Screws. *Constr and Build Mater*, 95: 762-773, 2015.
- [5] T. Tannert, F. Lam, T. Vallee. Strength Prediction for Rounded Dovetail Connections Considering Size Effects. *J. Eng. Mech.*, 136(3): 358-366, 2010.
- [6] T. Claus, W. Seim. Development of the Multiple Tenon Timber Connection Based on Experimental Studies and FE Simulation. *Engineering Structures*, 173:331-339, 2018.
- [7] J. R. Brown, M. Li, F. Sarti. Structural Performance of CLT Shear Connections with Castellations and Angle Brackets. *Engineering Structures*, 240: 112346, 2021.
- [8] T. Schmidt, H. J. Blaß. Contact Joints in Engineered Products. In: WCTE, 2016.
- [9] Canadian Commission On Building And Fire Codes. “National Building Code of Canada: 2020,” March 28, 2022, v. 1, 792 p.; v. 2, 708 p.
- [10] B. Sharma, A. Gatóo, M. Bock & M. Ramage. Engineered bamboo for structural applications. *Construction and Building Materials*, 81, 66–73, 2015.
- [11] Forest Products Laboratory. Wood handbook—Wood as an engineering material (General Technical Report FPL-GTR-282; p. 543). Department of Agriculture, Forest Service, Forest Products Laboratory, 2021
- [12] Y. Diao, & C. Loss. Long-span CLT-glulam composite flooring system connected with bamboo-based shear connectors: Feasibility of design for assembly. CSCE 2021 Annual Conference, Whistler, BC, Canada, 2022
- [13] D. Huang, Y. Bian, A. Zhou, & B. Sheng. Experimental study on stress–strain relationships and failure mechanisms of parallel strand bamboo made from phyllostachys. *Construction and Building Materials*, 77, 130–138, 2015.
- [14] H. Li, Z. Qiu, G. Wu, D. Wei, R. Lorenzo, C. Yuan, H. Zhang, & R. Liu. Compression Behaviors of Parallel Bamboo Strand Lumber Under Static Loading. *Journal of Renewable Materials*, 7(7), 583–600, 2019.
- [15] H. Li, Q. Zhang, D. Huang, & A. J. Deeks. Compressive performance of laminated bamboo. *Composites Part B: Engineering*, 54, 319–328, 2013.
- [16] C. Hong, H. Li, Z. Xiong, R. Lorenzo, X. Li, & Z. Wang. Axial compressive behavior of laminated bamboo lumber columns with a chamfered section. *Structures*, 33, 678–692, 2021.
- [17] Z. Chen, E. Zhu, & J. Pan. Numerical simulation of wood mechanical properties under complex state of stress. *Chinese Journal of Computational Mechanics*, 28(4), 629–634, 2011.
- [18] S. Widehammar. Stress-strain relationships for spruce wood: Influence of strain rate, moisture content and loading direction. *Experimental Mechanics*, 44(1), 44–48, 2004.
- [19] S., Ellis, & P. Steiner. The behaviour of five wood species in compression. *IAWA Journal*, 23(2), 201–211, 2002.
- [20] Ansys® Academic Research Mechanical, Release 2021 R1, Ansys Innovation Courses, Contact Mechanics, ANSYS, Inc.
- [21] R. Masoudnia, A. Hashemi, P. Quenneville, M. Asce, S. Engineer, & G., Ipenz. Predicting the Effective Flange Width of a CLT Slab in Timber Composite Beams. *J. Struct. Eng.*, 18, 2018.
- [22] J. Negrão, & L. Jorge. CLT Structure for Long Span Floors and Roofs—Optimizing the Cross-Section Properties. 41st IAHS World Congress: Sustainability and Innovation for the Future, 10, 2016.
- [23] C. Zhang, X. Zheng, & F. Lam. Development of composite action in a new long-span timber composite floor: Full-scale experiment and analytical approach. *Engineering Structures*, 279, 115550, 2023.